Letters

A Battery/Ultracapacitor Hybrid Energy Storage System for Implementing the Power Management of Virtual Synchronous Generators

Jingyang Fang, Yi Tang, Hongchang Li, and Xiaoqiang Li

***Abstract*—Renewable energy sources (RESs) have been extensively integrated into modern power systems to meet the increasing worldwide energy demand as well as reduce greenhouse gas emission. As a result, the task of frequency regulation previously provided by synchronous generators is gradually taken over by power converters, which serve as the interface between the power grid and RESs. By regulating power converters as virtual synchronous generators (VSGs), they can exhibit similar frequency dynamic response. However, unlike synchronous generators, power converters are incapable of absorbing/delivering any kinetic energy, which necessitates extra energy storage systems (ESSs). Nonetheless, the implementation and coordination control of ESSs in VSGs have not been investigated by previous research. To fill this research gap, this letter proposes a hybrid ESS (HESS) consisting of a battery and an ultracapacitor to achieve the power management of VSGs. Through proper control, the ultracapacitor automatically tackles the fast-varying power introduced by inertia emulation while the battery implements the remaining parts of a VSG and only compensates for relatively long-term power fluctuations with slow dynamics. In this way, the proposed HESS allows reduction of the battery power fluctuations along with its changing rate. Finally, experimental results are presented to validate the proposed concept.**

***Index Terms*—Battery, energy storage system (ESS), renewable energy source (RES), ultracapacitor (UC), virtual synchronous generator (VSG).**

I. Introduction

THE growing penetration of renewable energy sources (RESs) has redefined the operation of modern power systems [1]. In traditional power systems, synchronous generators are responsible for frequency regulation. During frequency events, they exhibit inertial response, which can slow down the frequency dynamics by absorbing or delivering the kinetic energy stored in the rotors of synchronous generators and turbines [2]. In future power systems, frequency regulation is supposed to be taken over by grid-connected power converters. However, conventional power converters are normally operated as current sources to extract the maximum power from RESs without providing any frequency regulation capability [1], [3].

An emerging concept for implementing frequency regulation is known as virtual synchronous generator (VSG) or virtual synchronous machine (VSM) [4]–[6]. The fundamental idea behind this concept lies in the emulation of synchronous generators through proper control of power converters. However, previous research works on VSGs or VSMs only focus on the controller design and rarely discuss the practical implementation of VSGs. In [6]–[9], the VSG is simply implemented by an ideal DC voltage source connected to an inverter. All the control loops in the VSG, e.g., inertia and speed governor, are realized by the ideal DC voltage source, which is obviously not the real case. In fact, energy storage systems (ESSs) must be involved in VSGs to achieve frequency regulation, and the implementation and coordination control of ESSs in VSGs have not been investigated in the literature.

For selection of energy storage units in an ESS, it is highly desirable that high energy density units can be used together with high-power density units to increase the system operating efficiency and/or lifetime as well as reduce system costs. One such example is the battery/ultracapacitor hybrid energy storage system (HESS), where the battery is used for compensation of low-frequency power fluctuations and the ultracapacitor is used for compensation of high-frequency power fluctuations [10]–[14]. To fully exploit the advantages of different energy storage units, low-/high-pass filters are normally employed to extract low-/high-frequency power fluctuations in the system. However, there is no guideline on how to design the cut-off frequency of such filters and it is typically determined through trial and error [12]–[14].

In view of these issues, this letter proposes a battery/ultracapacitor HESS to achieve the power management of VSGs. Specifically, the ultracapacitor is used to emulate the inertia of a VSG, as this part of the VSG is designed to cope with high-frequency power fluctuations. The remaining parts of the VSG, e.g., droop control and reheat turbine model, are emulated by the battery, as they are tasked at compensating for relatively long-term power fluctuations with slow dynamics. In this case, one can fully utilize the advantages of the ultracapacitor and battery to realize a practical VSG system. Moreover, since the HESS is used to emulate the inertia coefficient, droop

Manuscript received July 14, 2017; revised August 31, 2017 and September 21, 2017; accepted October 1, 2017. Date of publication October 5, 2017; date of current version January 3, 2018. This work was supported by the National Research Foundation, Prime Minister's Office, Singapore under the Energy Program and administrated by the Energy Market Authority under Award NRF2015EWT-EIRP002-007. *(Corresponding author: Yi Tang.)*

J. Fang, Y. Tang, and X. Li are with the School of Electrical and Electronic Engineering, Nanyang Technological University, Singapore 639798 (e-mail: jfang006@e.ntu.edu.sg; yitang@ntu.edu.sg; lixiaoqiang@ntu.edu.sg).

H. Li is with the Energy Research Institute, Nanyang Technological University, Singapore 639798 (e-mail: hongchangli@ntu.edu.sg).

Color versions of one or more of the figures in this letter are available online at http://ieeexplore.ieee.org.

Digital Object Identifier 10.1109/TPEL.2017.2759256

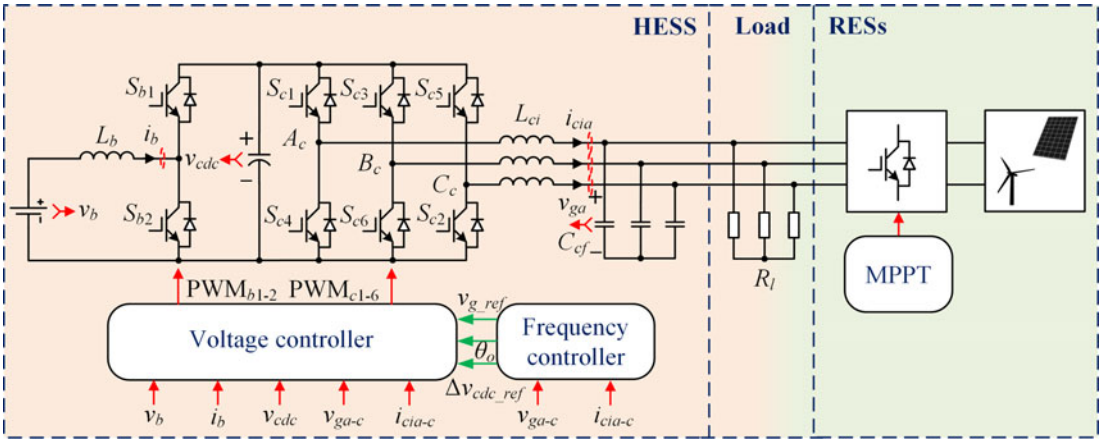

Fig. 1. Schematic diagram of the proposed VSG system.

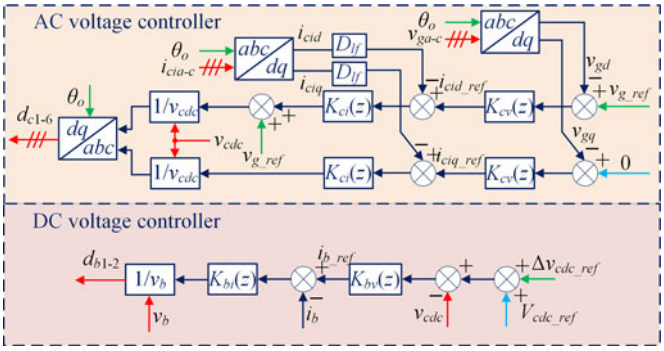

Fig. 2. Control block diagrams of the voltage controller.

control, speed governor, and turbine of a VSG, the control parameters for the HESS can easily be designed based on the VSG model. The power references of the ultracapacitor and battery are respectively derived from the virtual inertia emulation and the remaining parts of VSG control rather than conventional low-/high-pass filters. In Section II, the system schematic diagram is presented. Next, the power management scheme is detailed in Section III. Experimental results are provided in Section IV. Finally, Section V concludes the main contribution of this letter.

II. System Schematic Diagram

Conventionally, the VSG system is simply implemented by an ideal DC voltage source connected to an inverter. By controlling the inverter to mimic the operation of synchronous generators, the objective of frequency regulation can be achieved [6]–[9]. However, the ESS included in the VSG system is always neglected. In contrast, Fig. 1 illustrates the schematic diagram of the proposed system, where frequency regulation is implemented by a battery/ultracapacitor HESS. The battery is connected to the ultracapacitor through a DC/DC converter, and an *LC*-filtered three-phase inverter is employed as the interface between the ultracapacitor and AC load. Fig. 1 presents the simplest implementation of a HESS and other candidate topologies for such a system can be found in [10].

In Fig. 1, the voltage controller is dictated to follow the voltage references given by the frequency controller. Fig. 2 shows the control block diagrams of the voltage controller. It is noticed that the voltage controller consists of two separate parts, i.e., an AC voltage controller and a DC voltage controller. The AC voltage controller performs the regulation of the three-phase AC output voltages $v_{gi}\,(i = a, b, c)$ in the synchronous d–q frame while the DC-link voltage v_{cdc}, namely the voltage of the ultracapacitor, is controlled by the DC voltage controller. Both controllers are constructed following the standard cascaded control structure, which includes an inner current-loop and an outer voltage-loop [3].

The detailed control block diagram of the frequency controller is illustrated in Fig. 3, where the subscripts *pu* and *ref* stand for the per-unit and reference values, f_o, ω_o, and θ_o are respectively the output frequency, angular frequency, and displacement angle, f_g, P_g, and Q_g are respectively the measured grid frequency, active power, and reactive power.

This frequency controller functions similarly to the standard frequency regulator of synchronous generators, which can be found from page 598 to page 601 in [2]. In Fig. 3, R_d denotes the droop-coefficient, and the transfer function $K_p(s)$ models the dynamics of the speed governor and reheat turbine. Additionally, the DC-link voltage reference $\Delta v_{cdc\_ref\_pu}$ is dynamically adjusted according to the system frequency deviation Δf_{g_pu} through a gain K_{fv}, and then Δv_{cdc_ref} will be sent to the DC voltage controller shown in Fig. 2. Through this method, the power allocation between the battery and ultracapacitor can be achieved and will be explained in the next section.

III. Power Management Scheme

Fig. 4 visualizes the principle of the proposed power management scheme. Since frequency regulation is mainly determined by active power, the control blocks concerning reactive power are ignored here. From Fig. 4(a), the following well known swing equation can be obtained [2]:

$$\Delta P_{in\_pu} - \Delta P_{g\_pu} = D\Delta f_{g\_pu} + 2H\frac{d\Delta f_{g\_pu}}{dt} \tag{1}$$

or

$$\Delta P_{g\_pu} + \Delta P_{d\_pu} = \underbrace{\Delta P_{in\_pu}}_{\text{Battery}} + \underbrace{\left(-2H\frac{d\Delta f_{g\_pu}}{dt}\right)}_{\text{Ultracapacitor}} \tag{2}$$

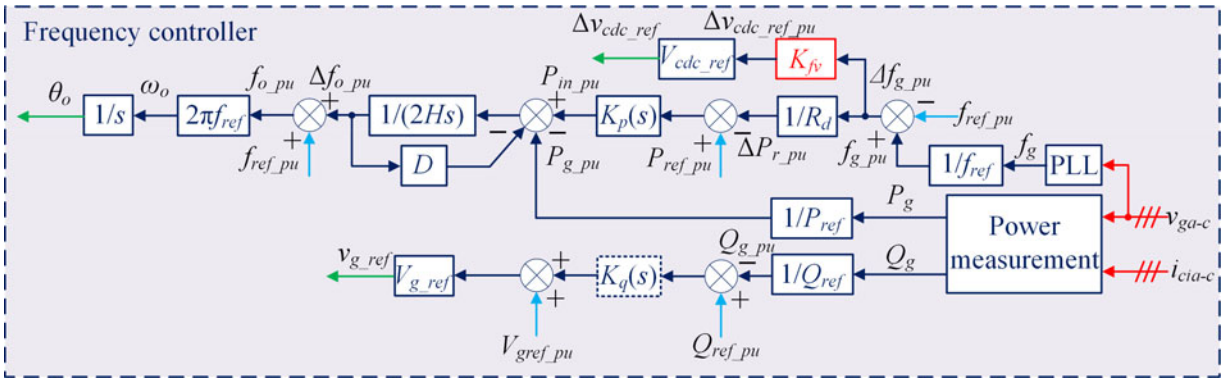

Fig. 3. Control block diagram of the frequency controller.

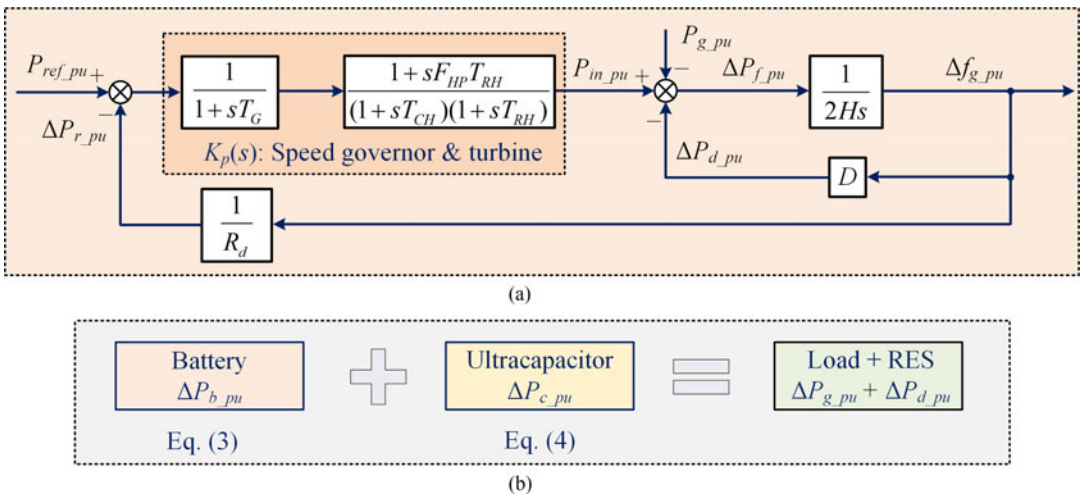

Fig. 4. Principle of the proposed power management scheme. (a) Frequency regulation framework. (b) Power allocation based on (2).

where ΔP_{g_pu} is the power variation caused by the load and RES and $\Delta P_{d\_pu} = D\Delta f_{g\_pu}$ is the power variation caused by the frequency-dependent load. $(\Delta P_{in\_pu} - 2Hd\Delta f_{g\_pu}/dt)$ is the power change of the VSG used for balancing the load and RES power variations in real time. As shown in Fig. 4(a), ΔP_{in_pu} should follow the power reference given by the frequency-droop $-\Delta P_{r\_pu}$, and it changes slowly due to the time delay introduced by the speed governor and turbine $K_p(s)$. ΔP_{in_pu} equals $-\Delta f_{g\_pu}/R_d$ in the steady-state. $-2Hd\Delta f_{g\_pu}/dt$ is the VSG power contributed by inertia emulation. This term varies very fast as it is in proportion to the time derivative of frequency. The fundamental idea behind the proposed power management scheme is to allocate fast-varying $-2Hd\Delta f_{g\_pu}/dt$ to the ultracapacitor and the slowly-changing ΔP_{in_pu} to the battery so that the advantages of these energy storage units can fully be utilized. The following equations should be satisfied to achieve this objective:

$$\Delta P_{b\_pu} = \Delta P_{in\_pu} = -\frac{\Delta f_{g\_pu}}{R_d} * K_p(t) \tag{3}$$

$$\Delta P_{c\_pu} = -2H\frac{d\Delta f_{g\_pu}}{dt} \tag{4}$$

where "$*$" stands for the convolution operation, $K_p(t)$ denotes the time-domain expression of $K_p(s)$, and ΔP_{b_pu} and ΔP_{c_pu} respectively represent the power changes of the battery and ultracapacitor, as shown in Fig. 4(b). ΔP_{c_pu} can alternatively be expressed as the following equation by differentiating the energy stored in the ultracapacitor:

$$\begin{aligned}\Delta P_{c\_pu} &= -\frac{1}{P_{ref}}\cdot\frac{d[0.5C_{dc}(V_{cdc\_ref}+\Delta v_{cdc})^2]}{dt}\\ &= -\frac{C_{dc}V_{cdc\_ref}}{P_{ref}}\cdot\frac{d\Delta v_{cdc}}{dt} = -\frac{C_{dc}{V_{cdc\_ref}}^2}{P_{ref}}\cdot\frac{d\Delta v_{cdc\_pu}}{dt}\\ &= -2H_c\frac{d\Delta v_{cdc\_pu}}{dt}\end{aligned} \tag{5}$$

where $H_c = 0.5C_{dc}{V_{cdc\_ref}}^2/P_{ref}$ represents the inertia coefficient of the ultracapacitor, P_{ref} stands for the system rated power used for normalization, and the capacitor voltage deviation is also normalized by $\Delta v_{cdc} = V_{cdc\_ref}\Delta v_{cdc\_pu}$. Since Δv_{cdc_pu} is related to Δf_{g_pu} with $\Delta v_{cdc\_pu} = K_{fv}\Delta f_{g\_pu}$ as defined by the frequency controller, shown in Fig. 3, ΔP_{c_pu} can be expressed as

$$\begin{aligned}\Delta P_{c\_pu} &= -2H_c\frac{d\Delta v_{cdc\_pu}}{dt} = -2K_{fv}H_c\frac{d\Delta f_{g\_pu}}{dt}\\ &= -2H\frac{d\Delta f_{g\_pu}}{dt} \Rightarrow H = K_{fv}H_c.\end{aligned} \tag{6}$$

TABLE I
SYSTEM AND CONTROL PARAMETER VALUES

Description	System parameter		Description	Control parameter	
	Symbol	Value		Symbol	Value
Battery voltage reference	V_{b_ref}	250 V	Frequency-droop coefficient	R_d	0.05
DC filter inductance	L_b	5.6 mH	Speed governor coefficient	T_G	0.1 s
DC-link voltage reference	V_{cdc_ref}	400 V	Turbine HP coefficient	F_{HP}	0.3 s
DC-link capacitance	C_{dc}	3.76 mF	Time constant of reheater	T_{RH}	7.0 s
AC filter inductance	L_{ci}	1 mH	Time constant of main inlet volumes	T_{CH}	0.2 s
AC filter capacitance	C_{cf}	50 μF	Inertia coefficient	H	5.0 s
Frequency reference	f_{ref}	50 Hz	Load damping coefficient	D	1.0
Maximum frequency deviation	Δf_{max}	0.2 Hz	Reactive power controller	$K_q(s)$	0
Maximum DC-link voltage deviation	Δv_{cdc_max}	27 V	Frequency-voltage gain	K_{fv}	16.6
Active power reference	P_{ref}	1 kW	UC inertia coefficient	H_c	0.3 s
Gird voltage reference	V_{g_ref}	110 V rms	Per-unit reference	P / Q / V / f_{ref_pu}	1.0

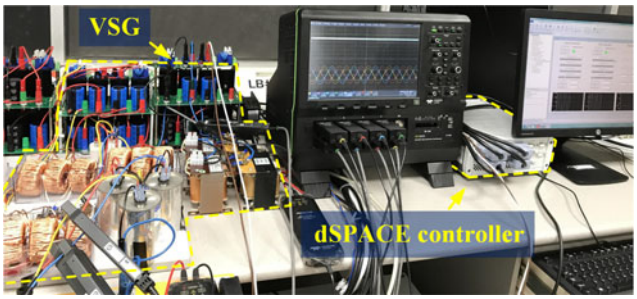

Fig. 5. Photo of the experimental test-bed.

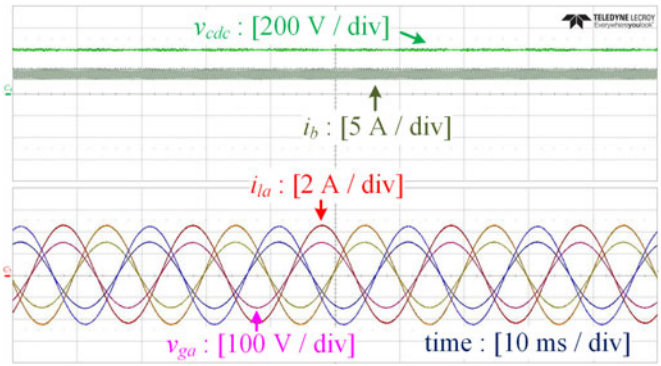

Fig. 6. Steady-state experimental waveforms of the proposed VSG system.

From (6), the desired proportional gain K_{fv} can be derived as

$$K_{fv} = \frac{2HP_{ref}}{C_{dc}V_{cdc\_ref}{}^2}. \tag{7}$$

It should be noted that the maximum value of K_{fv} depends on the allowable deviations of the DC-link voltage and system frequency [15]. To ensure linear modulation and avoid overstresses of semiconductors, a less than 15% DC-link voltage deviation is desired. Based on the above analysis, the control parameter values can be derived from the system parameter values and listed in Table I, where the emulated power system inertia H is designed to be 5, which is similar to the inertia constant of a conventional power system [2].

IV. EXPERIMENTAL VERIFICATION

Experiments were carried out based on the system schematic diagram shown in Fig. 1. A photo of the experimental test-bed is shown in Fig. 5. The control algorithms were executed on a dSPACE controller (Microlabbox), and an eight-channel oscilloscope (TELEDYNE LECROY: HDO8038) was used to capture the experimental waveforms.

Fig. 6 presents the steady-state experimental results of the proposed VSG system. As expected, the waveforms of the AC voltages v_{gi} $(i = a, b, c)$ are controlled as clean sinusoidal while the DC-link voltage v_{cdc} is maintained as a constant 400 V, thereby proving the effectiveness of voltage control.

Fig. 7 illustrates the system frequency response under a 3% step-up load change. It can clearly be observed that the VSG

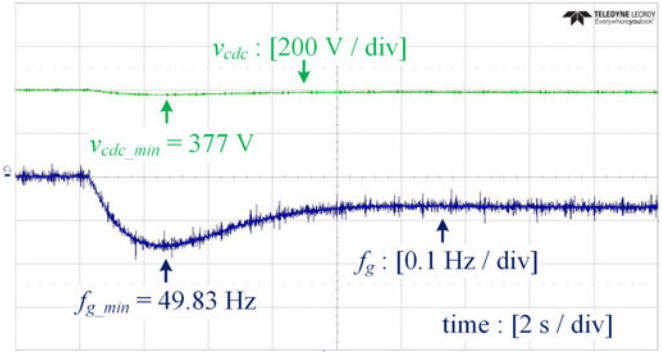

Fig. 7. System frequency responses under a 3% step-up load change.

exhibits similar inertial frequency response as conventional synchronous generators under this frequency event. Moreover, the DC-link voltage v_{cdc} tightly tracks its reference and varies in proportion to the system frequency f_g. As above-mentioned, the variation of v_{cdc} achieves the delivery of the inertial power. As a result, only the slowly-changing power is handled by the battery. It should be noted that a control mechanism can be implemented to restore the system frequency to its nominal value. In practice, this objective is achieved by the secondary frequency regulation, which is essentially an integrator with the frequency deviation as its input and the generation set-point as its output. Since this control loop is of slow response and has a large time

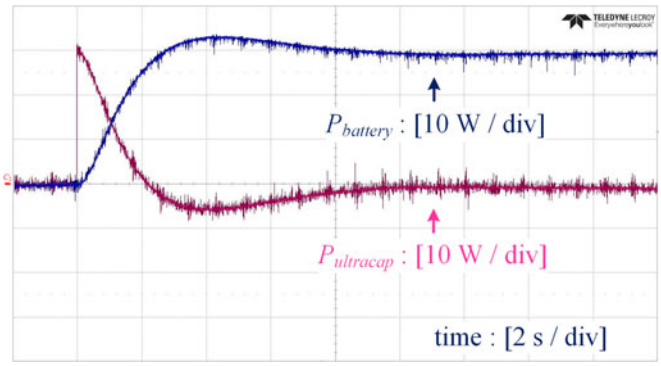

Fig. 8. System power responses under a 3% step-up load change.

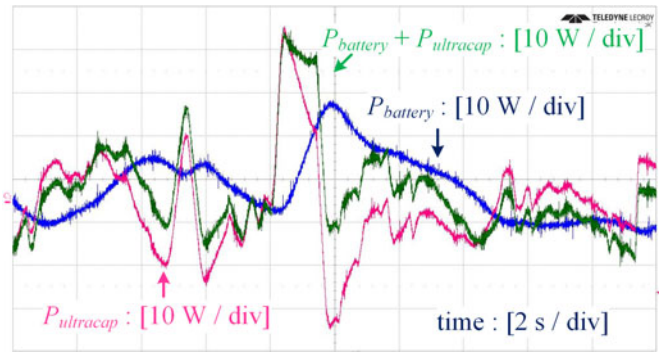

Fig. 9. System power responses under an intermittent RES output.

constant, it is normally achieved by conventional synchronous generators or batteries with high energy capacity.

The effectiveness of the proposed power management scheme is validated by Fig. 8, where the power allocation between the ultracapacitor and battery under the same 3% step-up load change is illustrated. As seen, the ultracapacitor responds promptly to the frequency event, which allows smooth discharge of the battery.

Fig. 9 further demonstrates the performance of the HESS under an intermittent RES output, where the power data was randomly generated to validate the power allocation of the proposed HESS-based VSG. A ramp rate limit of $\pm 10\%$ per second was applied when generating the data set according to [16]. Under this scenario, the high-frequency power disturbances can again be compensated by the ultracapacitor, and the power fluctuations of the battery can be reduced, which is consistent with the theoretical analysis. It should be mentioned that the battery power fluctuations can further be reduced by tuning the HESS controller. One possible solution is to increase the inertia coefficient H so that the frequency deviation Δf_g becomes smaller under the same intermittent RES output. However, this can only be achieved at the expense of the increased size of the ultracapacitor, because the emulated inertia is proportional to the energy stored in the ultracapacitor as indicated by (5).

V. Conclusion

This letter has proposed a battery/ultracapacitor HESS to implement VSGs as different energy storage units are suitable for different control tasks in the VSG. The ultracapacitor is used to emulate the inertia of a VSG and cope with high-frequency power fluctuations, while the battery is used to emulate the remaining parts of the VSG, e.g., droop control and reheat turbine model, to compensate for relatively long-term power fluctuations with slow dynamics. In this case, the power fluctuations of the battery along with its changing rate can dramatically be reduced. Since the HESS is used to emulate the inertia coefficient, droop control, speed governor, and turbine in a VSG model, which are all well known parameters, the controller design of the HESS is very straightforward and does not rely on the conventional low-/high-pass filters. Experimental results are presented to prove the effectiveness of the proposed HESS-based VSG.

References

[1] J. Rocabert, A. Luna, F. Blaabjerg, and P. Rodriguez, "Control of power converters in AC microgrids," *IEEE Trans. Power Electron.*, vol. 27, no. 11, pp. 4734–4749, Nov. 2012, doi: 10.1109/TPEL.2012.2199334.

[2] P. Kundur, *Power System Stability and Control*, New York, NY, USA: McGraw-Hill, 1994.

[3] F. Blaabjerg, R. Teodorescu, M. Liserre, and A. V. Timbus, "Overview of control and grid synchronization for distributed power generation systems," *IEEE Trans. Ind. Electron.*, vol. 53, no. 5, pp. 1398–1409, Oct. 2006, doi: 10.1109/TIE.2006.881997.

[4] J. Driesen and K. Visscher, "Virtual synchronous generators," in *Proc. IEEE Power Energy Soc. Gen. Meeting—Convers. Del. Elect. Energy 21st Century*, Jul. 2008, pp. 1–3, doi: 10.1109/PES.2008.4596800.

[5] H.-P. Beck and R. Hesse, "Virtual synchronous machine," in *Proc. 9th Int. Conf. Elect. Power Qual. Utilization*, 2007, pp. 1–6, doi: 10.1109/EPQU.2007.4424220.

[6] Q. Zhong and G. Weiss, "Synchronverters: Inverters that mimic synchronous generators," *IEEE Trans. Ind. Electron.*, vol. 58, no. 4, pp. 1259–1267, Apr. 2011, doi 10.1109/TIE.2010.2048839.

[7] J. Liu, Y. Miura, and T. Ise, "Comparison of dynamic characteristics between virtual synchronous generator and droop control in inverter-based distributed generators," *IEEE Trans. Power Electron.*, vol. 31, no. 5, pp. 3600–3611, May 2016, doi: 10.1109/TPEL.2015.2465852.

[8] J. A. Suul, S. D'Arco, and G. Guidi, "Virtual synchronous machine-based control of a single-phase bi-directional battery charger for providing vehicle-to-grid services," *IEEE Trans. Ind. Appl.*, vol. 52, no. 4, pp. 3234–3244, Jul./Aug. 2016, doi: 10.1109/TIA.2016.2550588.

[9] M. Guan, W. Pan, J. Zhang, Q. Hao, J. Cheng, and X. Zheng, "Synchronous generator emulation control strategy for voltage source converter (VSC) stations," *IEEE Trans. Power Syst.*, vol. 30, no. 6, pp. 3093–3101, Nov. 2015, doi: 10.1109/TPWRS.2014.2384498.

[10] S. M. Lukic, J. Cao, R. C. Bansal, F. Rodriguez, and A. Emadi, "Energy storage systems for automobile applications," *IEEE Trans. Ind. Electron.*, vol. 55, no. 6, pp. 2258–2267, Jun. 2008, doi: 10.1109/TIE.2008.918390.

[11] A. Khaligh and Z. Li, "Battery, ultracapacitor, hybrid energy storage systems for electric, hybrid electric, fuel cell, and plug-in hybrid electric vehicles: State of the art" *IEEE Trans. Veh. Technol.*, vol. 59, no. 6, pp. 2806–2814, Jul. 2010, doi: 10.1109/TVT.2010.2047877.

[12] J. Cao and A. Emadi, "A new battery/ultracapacitor hybrid energy storage system for electric, hybrid, and plug-in hybrid electric vehicles," *IEEE Trans. Power Electron.*, vol. 27, no. 1, pp. 122–132, Jan. 2012, doi: 10.1109/TPEL.2011.2151206.

[13] D. B. W. Abeywardana, B. Hredzak, V. G. Agelidis, and G. D. Demetriades, "Supercapacitor sizing method for energy-controlled filter-based hybrid energy storage system," *IEEE Trans. Power Electron.*, vol. 32, no. 2, pp. 1626–1637, Feb. 2017, doi: 10.1109/TPEL.2016.2552198.

[14] H. Zhou, T. Bhattacharya, D. Tran, T. S. T. Siew, and A. M. Khambadkone, "Composite energy storage system involving battery and ultracapacitor with dynamic energy management in microgrid applications," *IEEE Trans. Power Electron.*, vol. 26, no. 3, pp. 923–930, Mar. 2011, doi: 10.1109/TPEL.2010.2095040.

[15] J. Fang, X. Li, and Y. Tang, "Grid-connected power converters with distributed virtual power system inertia," in *Proc. 2017 IEEE Energy Convers. Congr. Expo.*, to be published.

[16] A. Ellis, D. Schoenwald, J. Hawkins, S. Willard, and B. Arellano, "PV output smoothing with energy storage," in *Proc. 2012 38th IEEE Photovolt. Spec. Conf.*, 2012, pp. 1523–1528, doi: 10.1109/PVSC.2012.6317885.